MNRAS 000, 1–19 (2019) Preprint 15 November 2019 Compiled using MNRAS LATEX style file v3.0

# The MUSE Atlas of Disks (MAD): Ionized gas kinematic maps and an application to Diffuse Ionized Gas.

Mark den Brok,[1,2★] C. Marcella Carollo,[1] Santiago Erroz-Ferrer,[1] Martina Fagioli,[3] Jarle Brinchmann,[4,5] Eric Emsellem,[6,7] Davor Krajnović,[2] Raffaella A. Marino,[1] Masato Onodera,[1,8] Sandro Tacchella,[1,9] Peter M. Weilbacher[2] and Joanna Woo[1,10]

[1] *Department of Physics, ETH Zürich, Wolfgang-Pauli-Str 27, 8093, Zürich, Switzerland*
[2] *Leibniz-Institut für Astrophysik Potsdam (AIP), An der Sternwarte 16, 14482 Potsdam, Germany*
[3] *Institute for Particle Physics and Astrophysics, ETH Zürich, Wolfgang-Pauli-Str 27, 8093, Zürich, Switzerland*
[4] *Instituto de Astrofísica e Ciências do Espaço, Universidade do Porto, CAUP, Rua das Estrelas, PT4150-762 Porto, Portugal*
[5] *Leiden Observatory, Leiden University, PO Box 9513, NL-2300 RA Leiden, the Netherlands*
[6] *European Southern Observatory, Karl-Schwarzchild-Str. 2, Garching bei München, 85748, Germany*
[7] *Univ Lyon, Univ Lyon1, ENS de Lyon, CNRS, Centre de Recherche Astrophysique de Lyon UMR5574, F-69230 Saint-Genis-Laval France*
[8] *Subaru Telescope, National Astronomical Observatory of Japan, HI 96720 Hilo, USA*
[9] *Harvard-Smithsonian Center for Astrophysics, 60 Garden St., Cambridge, MA 02138, USA*
[10] *Department of Physics & Astronomy, PO Box 1700 STN CSC, Victoria BC V8W 2Y2, Canada*



Accepted XXX. Received YYY; in original form ZZZ

**ABSTRACT**

We have obtained data for 41 star forming galaxies in the MUSE Atlas of Disks (MAD) survey with VLT/MUSE. These data allow us, at high resolution of a few 100 pc, to extract ionized gas kinematics $(V, \sigma)$ of the centers of nearby star forming galaxies spanning 3 dex in stellar mass. This paper outlines the methodology for measuring the ionized gas kinematics, which we will use in subsequent papers of this survey. We also show how the maps can be used to study the kinematics of diffuse ionized gas for galaxies of various inclinations and masses. Using two different methods to identify the diffuse ionized gas, we measure rotation velocities of this gas for a subsample of 6 galaxies. We find that the diffuse ionized gas rotates on average slower than the star forming gas with lags of 0-10 km/s while also having higher velocity dispersion. The magnitude of these lags is on average 5 km/s lower than observed velocity lags between ionized and molecular gas. Using Jeans models to interpret the lags in rotation velocity and the increase in velocity dispersion we show that most of the diffuse ionized gas kinematics are consistent with its emission originating from a somewhat thicker layer than the star forming gas, with a scale height that is lower than that of the stellar disk.

**Key words:** galaxies: spiral – galaxies: kinematics and dynamics

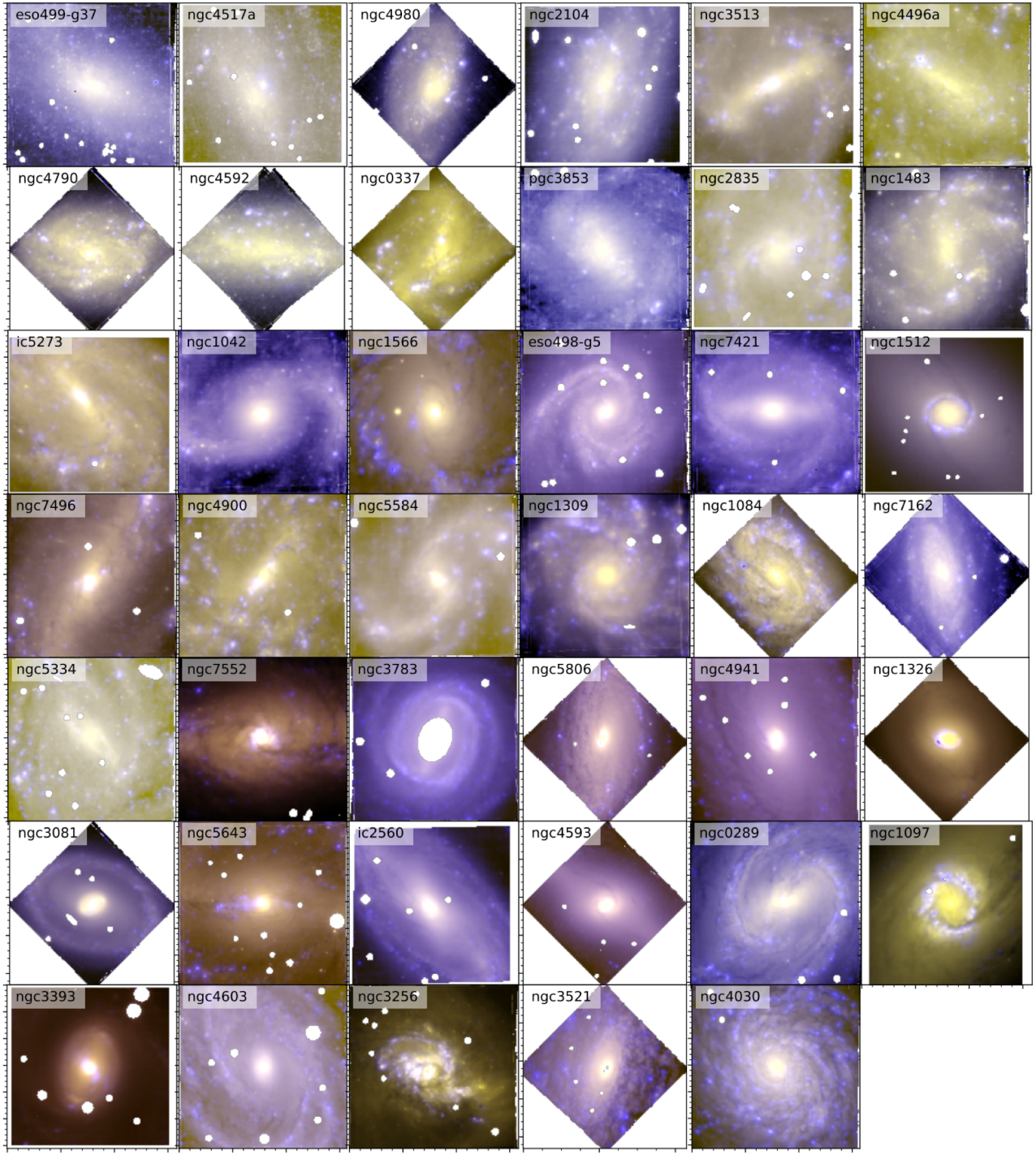
eso499-g37
ngc4517a
ngc4980
ngc2104
ngc3513
ngc4496a
ngc4790
ngc4592
ngc0337
pgc3853
ngc2835
ngc1483
ic5273
ngc1042
ngc1566
eso498-g5
ngc7421
ngc1512
ngc7496
ngc4900
ngc5584
ngc1309
ngc1084
ngc7162
ngc5334
ngc7552
ngc3783
ngc5806
ngc4941
ngc1326
ngc3081
ngc5643
ic2560
ngc4593
ngc0289
ngc1097
ngc3393
ngc4603
ngc3256
ngc3521
ngc4030

Отнаблюдали 45 галактик с MUSE.

Анализ:

- Voronoi binning по континууму => звездное население => вычитают из каждого пикселя
- Voronoi binning по Halpha => анализируют кинематику (отдельно Halpha+Hbeta, отдельно – все остальное)

| Name | Distance[Mpc] | $R_e$ [″] | $\log(M_\star/M_\odot)$ |
|---|---|---|---|
| ESO 499-G37 | 18.3 | 18.3 | 8.5 |
| NGC 4517A | 8.7 | 46.8 | 8.5 |
| NGC 4980 | 16.8 | 13.0 | 9.0 |
| NGC 2104 | 18.0 | 16.5 | 9.2 |
| NGC 3513 | 7.8 | 55.4 | 9.4 |
| NGC 4496A | 14.7 | 37.1 | 9.5 |
| NGC 4790 | 16.9 | 17.7 | 9.6 |
| NGC 4592 | 11.7 | 37.9 | 9.7 |
| NGC 337 | 18.9 | 24.6 | 9.8 |
| PGC 003853 | 11.3 | 73.1 | 9.8 |
| NGC 2835 | 8.8 | 57.4 | 9.8 |
| NGC 1483 | 24.4 | 19.0 | 9.8 |
| IC 5273 | 15.6 | 33.8 | 9.8 |
| NGC 1042 | 15.0 | 63.7 | 9.8 |
| NGC 1566 | 6.6 | 60.3 | 9.9 |
| ESO 498-G5 | 32.8 | 19.8 | 10.0 |
| NGC 7421 | 25.4 | 29.6 | 10.1 |
| NGC 1512 | 12.0 | 63.3 | 10.2 |
| NGC 7496 | 11.9 | 66.6 | 10.2 |
| NGC 4900 | 21.6 | 35.4 | 10.2 |
| NGC 5584 | 22.5 | 63.5 | 10.3 |
| NGC 1309 | 31.2 | 20.3 | 10.4 |
| NGC 1084 | 20.9 | 23.8 | 10.4 |
| NGC 7162 | 38.5 | 18.0 | 10.4 |
| NGC 5334 | 32.2 | 51.2 | 10.6 |
| NGC 7552 | 22.5 | 26.0 | 10.6 |
| NGC 3783 | 40.0 | 27.7 | 10.6 |
| NGC 5806 | 26.8 | 27.2 | 10.7 |
| NGC 4941 | 15.2 | 64.7 | 10.8 |
| NGC 1326 | 18.9 | 26.2 | 10.8 |
| NGC 3081 | 33.4 | 18.9 | 10.8 |
| NGC 5643 | 17.4 | 60.7 | 10.8 |
| IC 2560 | 32.2 | 37.7 | 10.9 |
| NGC 4593 | 25.6 | 63.3 | 11.0 |
| NGC 289 | 24.8 | 27.0 | 11.0 |
| NGC 1097 | 16.0 | 55.0 | 11.1 |
| NGC 3393 | 55.2 | 21.1 | 11.1 |
| NGC 4603 | 32.8 | 44.7 | 11.1 |
| NGC 3256 | 38.4 | 26.6 | 11.1 |
| NGC 3521 | 14.2 | 61.7 | 11.2 |
| NGC 4030 | 29.9 | 31.8 | 11.2 |

# Поля скоростей ионизованного газа

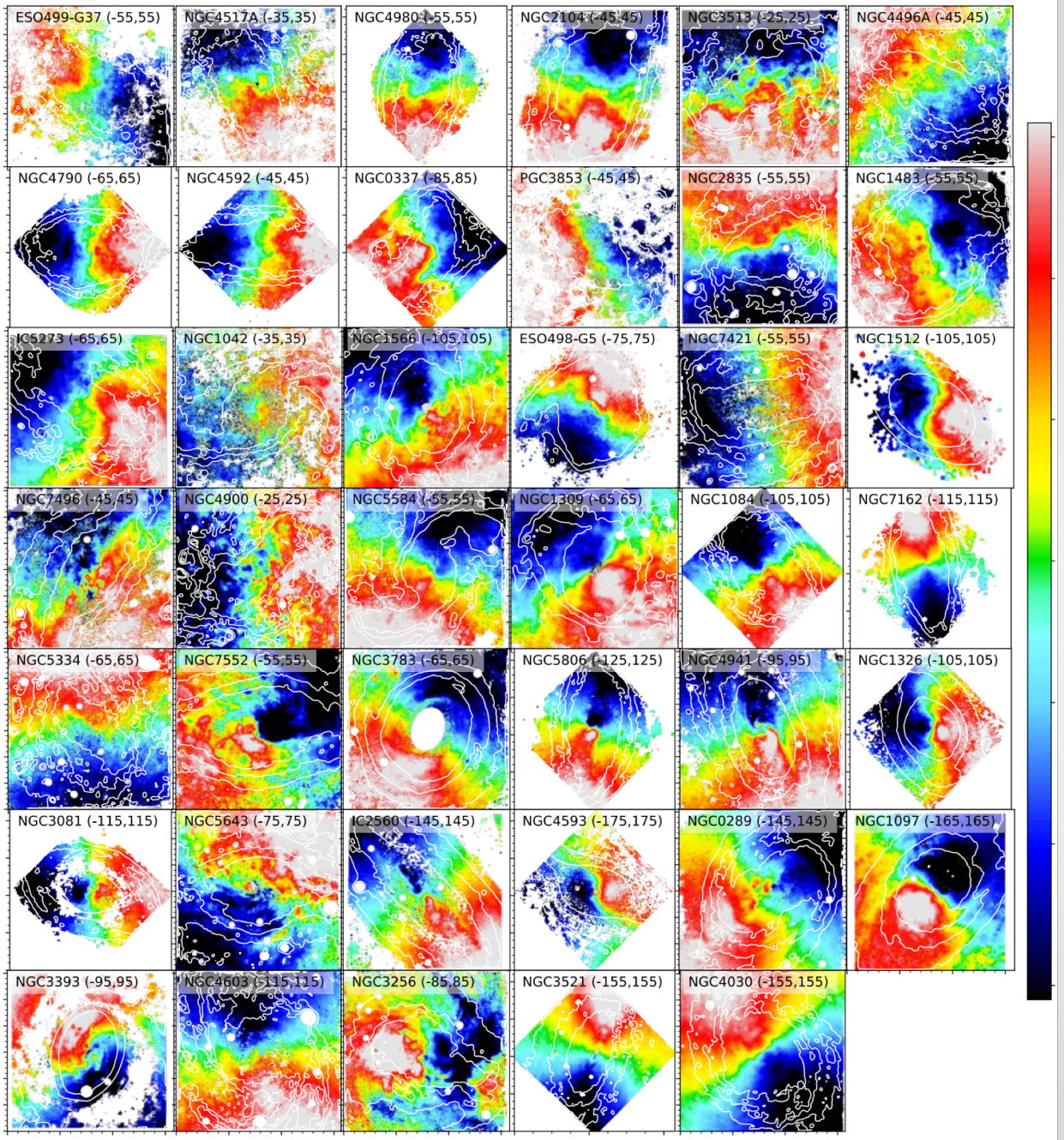


**Figure 2.** Maps of the velocity of the ionized gas derived from H$\alpha$ and H$\beta$. White contours trace the shape of the galaxy as seen in the white light image and are logarithmically spaced in brightness between the 30% and 95% brightness levels. North points up in every map.

# Поля дисперсии скоростей ионизованного газа

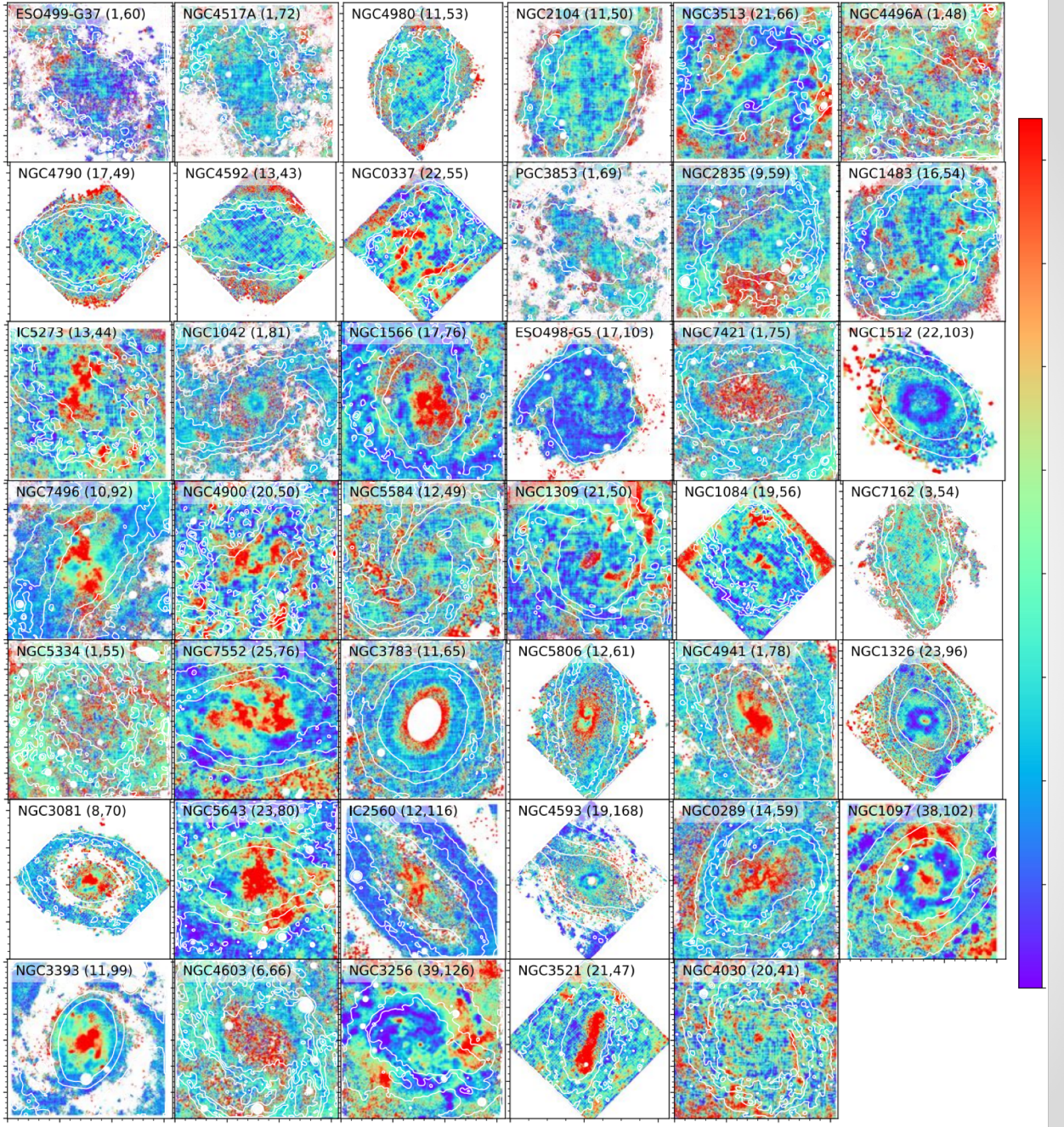


**Figure 3.** Maps of the dispersion of the ionized gas derived from H$\alpha$ and H$\beta$. Contours and image sizes as in Fig. 2. The colour scale is linear between the two numbers in brackets in km/s.

Цель работы – сравнительный анализ кинематики DIG и областей звездообразования.

| Galaxy | Classification | P.A. [deg] | q | $f_0$ [$10^{-20}$ erg s$^{-1}$cm$^{-2}$] |
|---|---|---|---|---|
| NGC 4790 | Sm sp | -4 | 0.73 | 1580.2 |
| NGC 4592 | SA(s)bc | 5 | 0.30 | 1329.9 |
| NGC 1084 | SA(s)c | -54 | 0.54 | 1632.3 |
| NGC 7162 | SAB(rs)bc | -80 | 0.42 | 476.0 |
| NGC 3521 | SA(r'l,r)bc | 255 | 0.45 | 1606.3 |
| NGC 4030 | SA(rs)bc | -54 | 0.78 | 1374.3 |

Два способа выделить DIG:

1) Blanc et al. (2009):
[S II]/H$\alpha$ = 0.35 для DIG; [S II]/H$\alpha$ = 0.11 для HII

2) Weilbacher et al. (2018):
Astrodendro

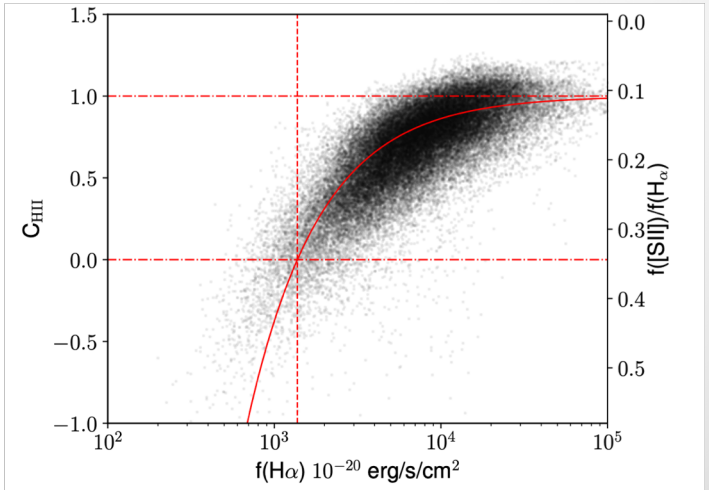


**Figure 4.** Ratio of [S II]/H$\alpha$ for spaxels in NGC 4030. The dash-dotted lines show the fitted values for the [S II]/H$\alpha$ ratio for pure H II regions (upper line) and for diffuse gas (lower line). The vertical dashed line shows the location of $f_0$ (see text).

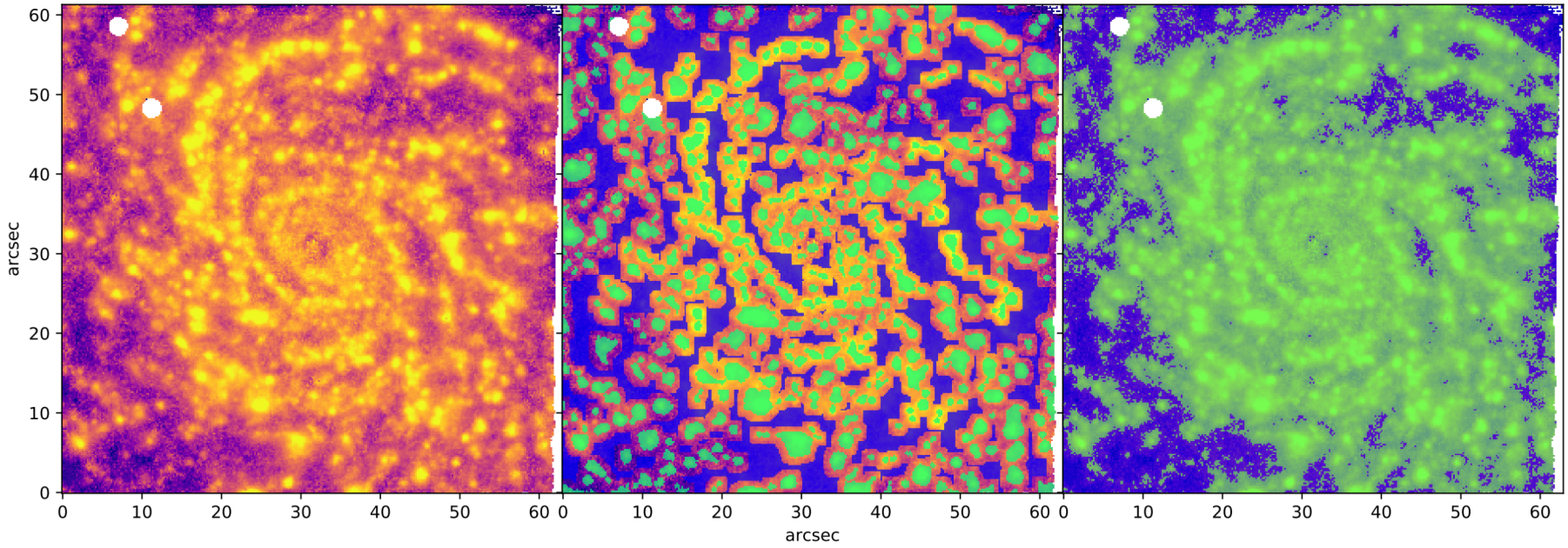


**Figure 5.** Identification of DIG and SF gas for NGC 4030. The left panel shows the H$\alpha$ map of NGC 4030. In the middle panel (dendrogram method) and right panel (Blanc method), the SF and DIG gas are identified as bright green and blue, while fully transparent areas are excluded.

Второй метод дает вклад DIG порядка 30% в общий поток, что больше согласуется с оценками в других работах

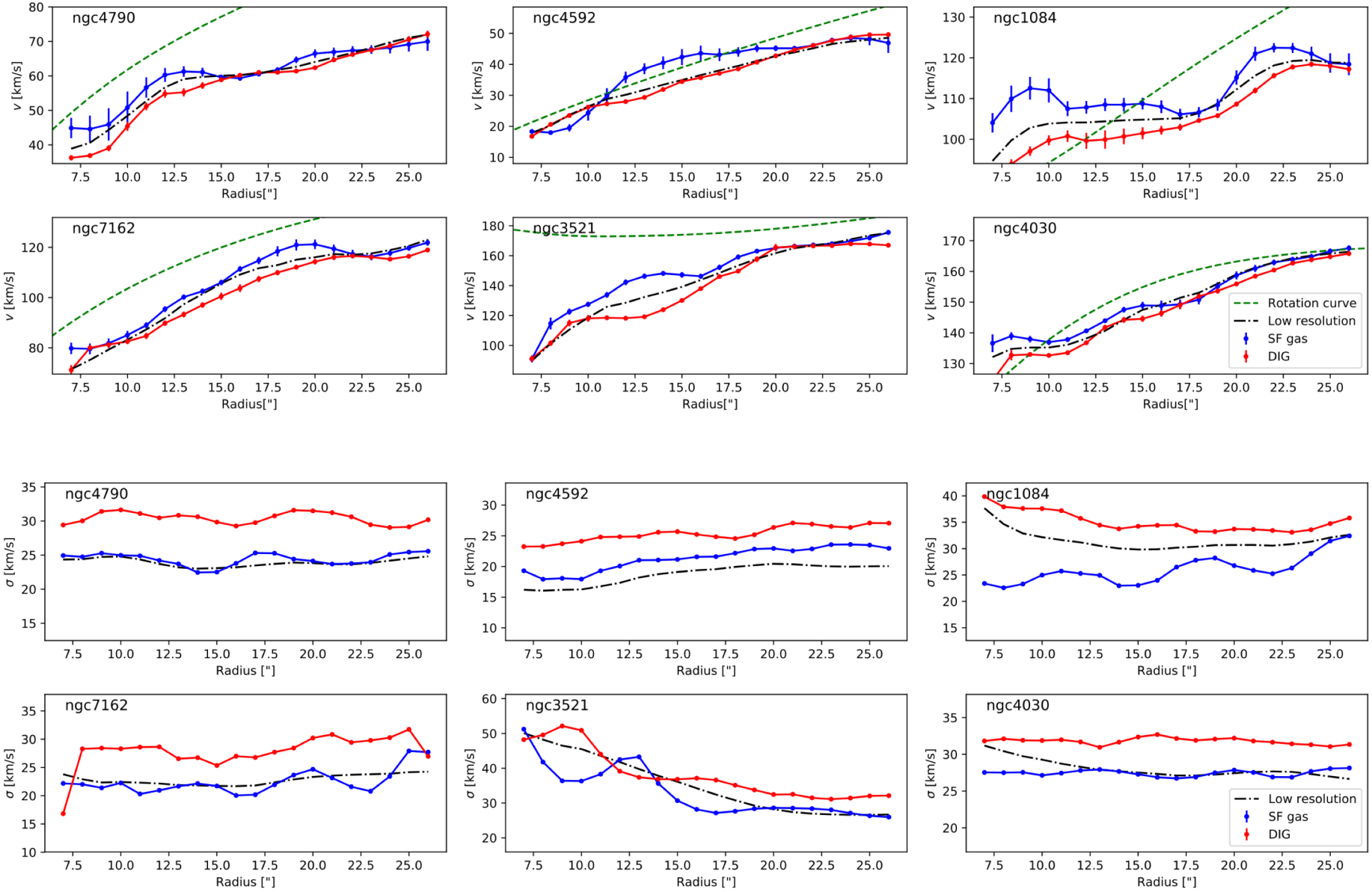


**Figure 6.** Rotation velocities (upper 6 panels) and velocity dispersion (lower 6 panels) of star forming and diffuse gas in a subset of the 6 most regularly rotating galaxies in our sample. Star forming gas is shown in blue, diffuse ionized gas in red. The low-resolution luminosity weighted quantities are shown in black dashed-dotted lines. Star forming and diffuse gas were separated by the dendrogram method. For completeness, we also indicate with green the circular velocity curve as derived from stellar kinematics (see Appendix D).

# Есть лаг между SF и DIG, особенно если выделять DIG по astrodendro

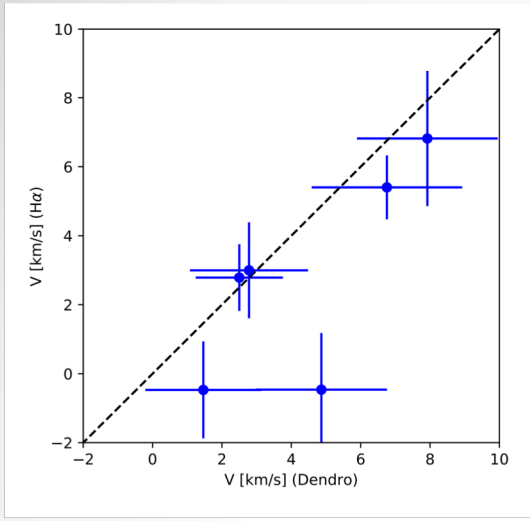


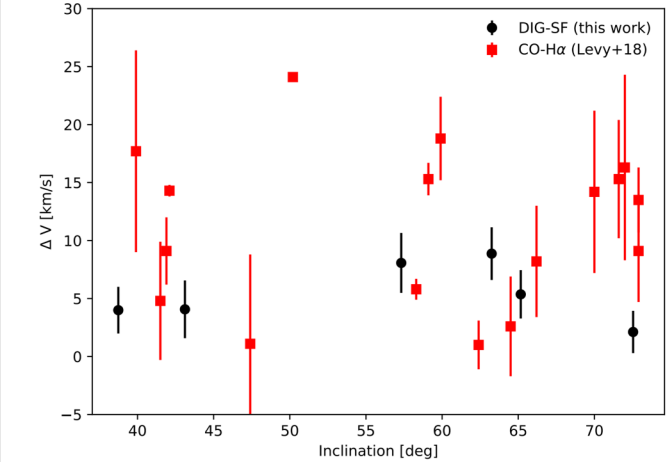


**Figure 10.** Median velocity differences for SF and DIG gas versus the inclination of the host galaxy (black). We also show the difference in CO velocity and H$\alpha$ velocity as determined by Levy et al.

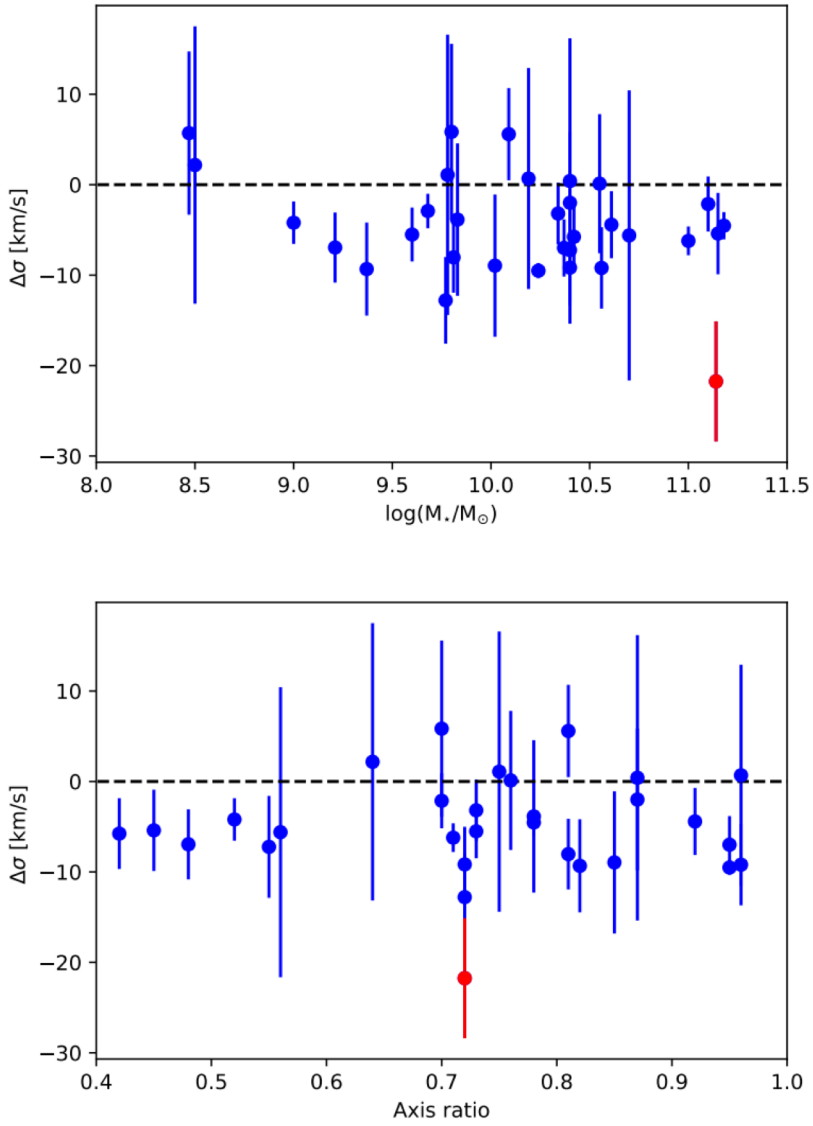


**Figure 9.** Median velocity dispersion differences for SF and DIG gas for the star forming sample as a function of stellar mass (upper panel) and axis ratio (lower panel). The red point is the merger remnant NGC 3256. A negative $\sigma$ means that the dispersion of the DIG is higher than that of the SF gas.

Результаты качественно не меняются, если скорость измерять по [NII]

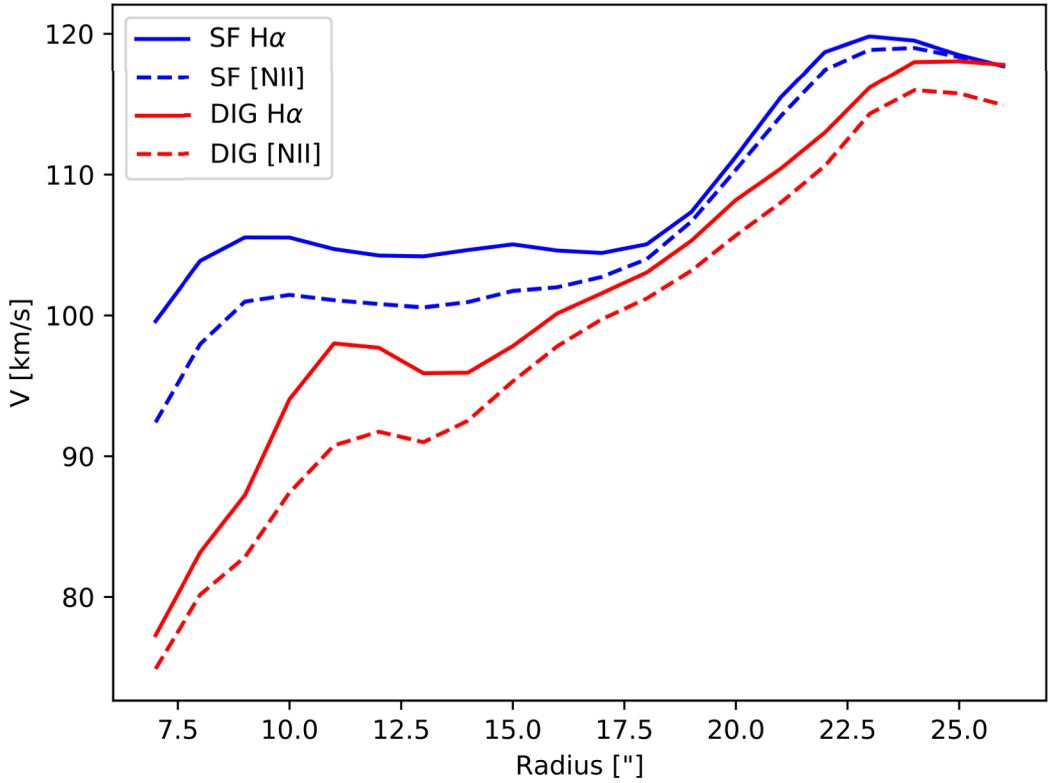


**Figure 11.** Comparison between the rotation velocities determined from the Balmer lines and the [N II] lines for NGC 1084. Star forming gas is shown in blue, DIG in red. Velocities derived from [N II] lines are dashed.

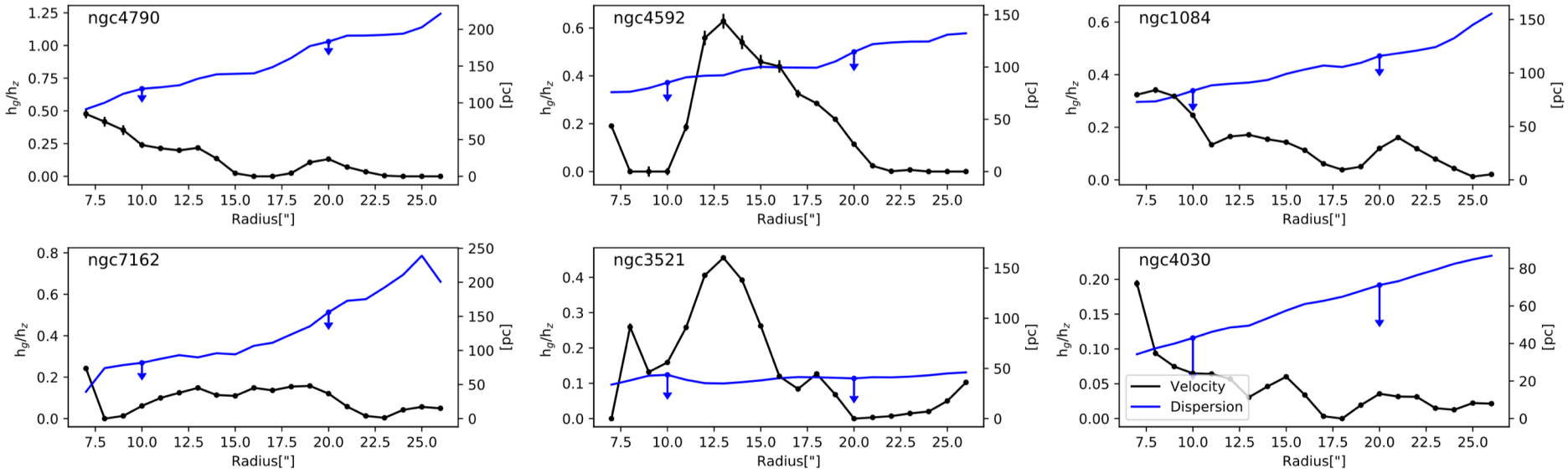


**Figure 12.** Radially varying scale heights of DIG as inferred from velocity differences (black) and dispersions (blue) with respect to the scale height of the stellar disk. The scale height in pc is given on the right axis. As the non-gravitational component of the dispersions is not known, the dispersion measurements are approximate upper limits.

Допустим, что DIG лежит над плоскостью диска, и его распределение описывается моделью Джинса. Тогда получается, что расположен он невысоко над диском

$$\sigma_z^2 = 2\pi G\Sigma(R)h_g\left[1-\frac{1}{(1+\frac{h_g}{h_z})^2}\right]. \qquad \text{(B5)}$$

$$\overline{V} = V_0\frac{1}{1+\frac{h_g}{2h_z}}. \qquad \text{(B7)}$$